

## Durham Research Online

---

### Deposited in DRO:

10 January 2018

### Version of attached file:

Accepted Version

### Peer-review status of attached file:

Peer-reviewed

### Citation for published item:

Hizzett, J. L. and Hughes Clarke, J. E. and Sumner, E. J. and Cartigny, M. J. B. and Talling, P. J. and Clare, M. A. (2018) 'Which triggers produce the most erosive, frequent and longest runout turbidity currents on deltas?', *Geophysical research letters.*, 45 (2). pp. 855-863.

### Further information on publisher's website:

<https://doi.org/10.1002/2017gl075751>

### Publisher's copyright statement:

©2017. The Authors. This is an open access article under the terms of the Creative Commons Attribution License, which permits use, distribution and reproduction in any medium, provided the original work is properly cited.

### Additional information:

---

## Use policy

The full-text may be used and/or reproduced, and given to third parties in any format or medium, without prior permission or charge, for personal research or study, educational, or not-for-profit purposes provided that:

- a full bibliographic reference is made to the original source
- a [link](#) is made to the metadata record in DRO
- the full-text is not changed in any way

The full-text must not be sold in any format or medium without the formal permission of the copyright holders.

Please consult the [full DRO policy](#) for further details.

# Which triggers produce the most erosive, frequent and longest runout turbidity currents on deltas?

Hizzett, J. L.<sup>1,4</sup>, Hughes Clarke, J. E.<sup>2</sup>, Sumner, E. J.<sup>1</sup>, Cartigny, M. J. B.<sup>3</sup>, Talling, P. J.<sup>3</sup>, and Clare, M. A.<sup>4</sup>.

<sup>1</sup> Ocean and Earth Science, National Oceanography Centre Southampton, University of Southampton, European Way, Southampton, SO14 3ZH, United Kingdom.

<sup>2</sup> Center for Coastal and Ocean Mapping, University of New Hampshire, 24 Colovos Road, Durham, New Hampshire 03824, USA.

<sup>3</sup> Departments of Earth Science and Geography, University of Durham, Durham, DH1 3LE, United Kingdom.

<sup>4</sup> National Oceanography Centre, University of Southampton Waterfront Campus, European Way, Southampton, SO14 3ZH, United Kingdom.

Corresponding author: Jamie L. Hizzett (J.L.Hizzett@soton.ac.uk)

## Key Points:

1. It was previously thought that landslides and plunging (hyperpycnal) floods dominate triggering of turbidity currents offshore deltas.
2. But the most detailed time-lapse mapping of a delta shows that turbidity currents linked to settling from surface river plumes may dominate.
3. Settling plume events can pose the greatest hazard, and make the greatest changes to delta morphology, at least over sub-annual time scales.

## Abstract

Subaerial rivers and turbidity currents are the two most voluminous sediment transport processes on our planet, and it is important to understand how they are linked offshore from river mouths. Previously it was thought that slope failures or direct plunging of river flood water (hyperpycnal flow) dominated the triggering of turbidity currents on delta-fronts. Here we re-analyse the most detailed time-lapse monitoring yet of a submerged delta; comprising 93 surveys of the Squamish Delta in British Columbia, Canada. We show that most turbidity currents are triggered by settling of sediment from dilute surface river plumes, rather than landslides or hyperpycnal flows. Turbidity currents triggered by settling plumes occur frequently, run out as far as landslide-triggered events, and cause the greatest changes to delta and lobe morphology. For the first time, we show that settling from surface plumes can dominate the triggering of hazardous submarine flows and offshore sediment fluxes.

This article has been accepted for publication and undergone full peer review but has not been through the copyediting, typesetting, pagination and proofreading process which may lead to differences between this version and the Version of Record. Please cite this article as doi: 10.1002/2017GL075751

## **1. Introduction**

River deltas play an important role in global carbon and sediment cycles. They receive much of the annual flux of 20 billion tonnes of fluvial sediments that either is stored in deltas or redistributed in the oceans (Milliman and Farnsworth, 2013). Fjords fed by river deltas store 11% of the carbon delivered by rivers to the ocean each year.

Sediment is redistributed over the submarine part of deltas by turbidity currents. Turbidity currents pose a hazard to subsea infrastructure such as cables and pipelines (Carter et al., 2014). Understanding how turbidity currents are triggered and evolve is key to linking fluvial sediments to their ultimate resting place in the world's oceans.

Here we seek to understand how turbidity currents are triggered offshore from river mouths, and which trigger mechanism produces the most frequent, erosive, and longest runout turbidity currents. These factors are particularly important because they determine which flows are the most hazardous, or transport the most sediment and cause the most seabed change, and thus play the greatest role in transforming deltas.

There are few direct observations of turbidity currents in action, and even fewer observations of multiple turbidity currents at one site with different triggers. This means that although a number of trigger mechanisms have been proposed, there are few field studies that document which triggers dominate and are associated with the largest sediment fluxes. In this study we analyse the most detailed time-lapse mapping yet from a deltaic system to understand how trigger mechanisms are linked to flow behaviour and runout. This dataset comprises 93 near-daily time lapse surveys acquired at Squamish Delta in Howe Sound, Canada, during the 2011 freshet. These surveys define 95 turbidity current events, recognised by changes in seafloor elevation, across the three channels (Fig. 1; Hughes Clarke et al., 2012; Hughes Clarke et al., 2014; Hughes Clarke, 2016).

We seek to understand the importance of turbidity currents formed by different trigger mechanisms at a fjord-head delta. Our aims are to: (1) Determine which is the most common trigger mechanism for turbidity currents; (2) Show which trigger mechanism generates turbidity currents that rework the most sediment and thus have the greatest effect on delta sculpting; (3) Determine which trigger mechanism produces the longest runout flows and carries the most sediment to the lobe.

### *1.1 Past work on turbidity current triggers on deltas*

Various processes have been proposed to trigger turbidity currents on deltas, these include: submarine landslides (Obelcz et al., 2017; Prior et al., 1981); plunging (hyperpycnal) river plumes (Dietrich et al., 2016; Mulder et al., 2003), sediment settling from surface (hypopycnal) river plumes (Kineke et al., 2000; Parsons et al., 2001), and by sediment remobilised by internal waves or tides (Normandeau et al., 2014; Saucier and Chassé, 2000).

Submarine slope failures (hereafter called 'landslides') can mix with seawater to generate more dilute turbidity currents that runout further than the toe of the landslide deposit. Landslides can occur due to over steepening of the prograding delta lip and can be released abruptly (Prior et al., 1981) or gradually by retrogressive breaching (Mastbergen and Van Den Berg, 2003). Landslides can transform into turbidity currents if the body of sediment disintegrates, enabling turbulence to suspend sediment (Felix and Peakall, 2006). The runout of landslide-triggered turbidity currents is poorly documented and understood. Large volume terrestrial landslides runout further than

small volume landslides (Dade and Huppert, 1998). However, it is unknown if the same relationship holds in the ocean where the flow can evolve and transform through water entrainment.

Hyperpycnal flows occur when rivers form a sediment-laden plume that is denser than the ambient seawater (Mulder and Syvitski, 1995). Such a hyperpycnal plume plunges beneath the seawater and flows along the basin floor as a turbidity current. Hyperpycnal flows in marine environments are thought to occur during river flood events when suspended sediment concentrations exceed  $\sim 40 \text{ kg m}^{-3}$  (Mulder et al., 2003). Hyperpycnal flows can erode sediment from the seafloor (Dietrich et al., 2016), thus enhancing their density contrast and leading to acceleration (Pantin, 1979; Parker et al., 1986).

Turbidity currents triggered by sediment settling from a river plume, hereafter called 'plume-triggered events', occur when sediment settles out from a buoyant surface (hypopycnal) plume onto the seafloor (Parsons et al., 2001). Sediment is initially concentrated in sheets or small-scale fingers at the base of the buoyant plume. This can lead to sediment concentrations that exceed  $20 \text{ kg m}^{-3}$ , and result in sediment settling (Parsons et al., 2001). Detailed field observations of plume events are rare (Lintern et al., 2016), but have shown that resulting flows can be fast moving ( $>10 \text{ ms}^{-1}$ ). Plume events are as yet an understudied phenomenon, and are documented by few field studies (e.g. Kineke et al., 2000; Hughes Clarke et al., 2014; Lintern et al., 2016) or inferred from numerical (Shao et al., 2017) and laboratory studies (Parsons et al., 2001; Sequeiros et al., 2009).

Once turbidity currents are triggered, they can evolve along three trajectories. In the first trajectory, (1) the flow erodes more sediment than it deposits leading to 'self' acceleration (Pantin, 1979; Parker et al., 1986). This increases flow density, and leads to acceleration of the flow, which in turn leads to further erosion. The second trajectory (2) leads to a dissipating flow (Pantin, 1979; Parker et al., 1986), where the flow deposits more sediment than it erodes. This net-deposition reduces the density contrast and the flow decelerates. The third trajectory (3) bypasses sediment causing near-equal amounts of sediment deposition and erosion. However, the relationship between triggering mechanism and subsequent flow evolution is poorly understood due to a lack of suitably detailed field observations.

## **2. Regional Background**

Squamish Delta is an example of a sandy fjord-head system in which water depths increase rapidly offshore to 100 m within  $\sim 1 \text{ km}$  of the shore (Hughes Clarke et al., 2014; Fig. 1a). The delta-front comprises three distinct channel-lobe systems with bedform fields (northern, central and southern channels; Fig. 1b) formed by turbidity currents (Hughes Clarke et al., 2012). The bedforms in each channel (interpreted as cyclic steps (Hughes Clarke et al., 2012)) interact with, and are maintained by, turbidity currents (Fig. 1c).

During the May-October freshet the Squamish River discharge exceeds  $350\text{--}500 \text{ m}^3 \text{ s}^{-1}$ , with occasional flood peaks in excess of  $1,000 \text{ m}^3 \text{ s}^{-1}$  (Clare et al., 2016; Hughes Clarke et al., 2014). Bedload from the gravelly riverbed flows over the delta-lip, sometimes causing progradation of  $>10 \text{ m}$  in a single day. However, much of the delta-front sediment is fine-to-medium sand, which is finer than the gravel-dominated bedload in the river channel. This suggests that the delta-front sediment mostly

originates from the ebb-tide river washload carried offshore in a surface plume (Hughes Clarke, 2016). Rapid ( $>3000 \text{ m}^3$  per low tide (Pratomo, 2016)) accumulation of sediment leads to slope failure (Hickin, 1989; Hughes Clarke et al., 2012), with the largest ( $50,000\text{--}150,000 \text{ m}^3$ ) delta-lip failures typically occurring a few hours after flood peaks (Clare et al., 2016). Suspended sediment measurements in the river plume show that sediment concentrations are insufficient (usually  $<0.07 \text{ kg m}^{-3}$ ) to form a plunging (hyperpycnal) flow (Hughes Clarke et al., 2014).

Hughes-Clarke et al. (2014) demonstrated that turbidity currents commonly occur at low tides due to sediment settling from the Squamish River plume. Sediment settling from the river plume was demonstrated by high backscatter both at the surface and in the water column (Supplemental Figure 2). Similar observations of plume-triggered turbidity currents have been made offshore from other rivers globally (e.g. Sepik River, Papua New Guinea (Kineke et al., 2000); Fraser River Delta, Canada (Ayranci et al., 2012; Kostaschuk et al., 1993; Lintern et al., 2016)). These observations are also in agreement with the experimental models of Parsons et al. (2001), which show that turbidity currents can be triggered by river plumes with densities below the threshold required for river plunging. Whilst the exact mechanism by which settling plume sediment generates turbidity currents is still poorly understood, it seems likely that this mechanism is more widespread than currently recognised due to the lack of appropriate monitoring data (Wright and Friedrichs, 2006). To determine whether conditions at the Squamish Delta are typical, we compare the suspended sediment flux, discharge and sediment yield with 566 other rivers in the global database (Supplemental Figure 1) of Peucker-Ehrenbrink (2009). The Squamish River, and other rivers where turbidity currents are known to be triggered by settling from river plumes (Fraser Delta, Sepik River), fit well within the broad spread of measurements. This suggests that settling plumes may also be likely in many other locations globally.

### **3. Methods**

Here we study the relationship between flow triggers and flow evolution. Both the type of trigger and how the flow evolves are deduced from changes in seafloor morphology (Fig 1c-e), between 93 sequential near-daily surveys. This allows us to define 95 turbidity currents that occurred across three channels on the delta front. We use this to understand flow runout and behaviour from patterns of erosion and deposition caused by these flows. We distinguish landslide-triggered flows, from flows that we infer to be triggered by sediment settling from surface plumes, using the presence or absence of a landslide head scar.

Data were collected using an EM710 multibeam sonar with a vertical resolution of 0.2% of water depth, and a horizontal resolution of 3% of water depth. The active prodelta region was surveyed every weekday, with the distal delta surveyed every fortnight. The very shallow water ( $< 5 \text{ m}$ ) delta top was also surveyed on a semi-weekly basis (Hughes Clarke et al., 2012).

We calculated the difference in seafloor elevation between consecutive bathymetric surveys, which are typically 1-day apart, but can be 3-days apart across weekends. We define an event when there is discernible change in seafloor morphology, and subdivide events that affected the southern, central and northern channels on the delta front. When there is change in more than one channel during the same period, these are counted as separate events. We note that more than one turbidity current or landslide may have occurred between consecutive surveys. Landslide volumes for surveys across

weekends are not significantly greater than those during weekdays, and the 3 largest landslides occurred between weekdays, suggesting that this variable time period between surveys is not causing detectable bias (Supplemental Figure 3).

Flows cause upstream migration of bedforms (Hughes Clarke et al., 2012; Hughes Clarke, 2016; Fig 1b). Such upslope migrating bedforms are represented in the difference map by adjacent patches of lee-side erosion and stoss-side deposition (Fig. 1c-e). If the volume of erosion on the lee slope exceeds deposition on the stoss slope, then this represents an overall increase in the volume of sediment within the turbidity current. If the erosion and deposition are almost equal, the flow is said to be bypassing as there is no net change in flow volume across one bedform. The evolution of the total amount of sediment in the turbidity current is then calculated by the cumulative loss and gain of sediment volumes with distance from the delta lip (Fig. 2a). For error estimations see Supplemental Figure 4.

The flow trigger is defined using the presence or absence of a visible head scar near the delta-lip in the difference maps, which typically have a vertical resolution of a few tens of centimetres. Given that events initiate in water depths below 60 m and the vertical resolution is 0.2% water depth, the worst-case-scenario is that a head scar thinner than 12 cm would not be recognised. As the delta-top was surveyed only every 3 or 4 days, this means that the headwall region of some landslides may not have been surveyed on some days, yielding an underestimation of initial landslide volume. This occurred for 6 out of a total of 26 landslide events (Figure 3).

Runout is measured as the distance from the first to last contour that shows discernible (typically  $>0.25$  m) bathymetric change (Fig. 1c-e). We note that flows may have runout further but failed to cause resolvable change to the sea floor. Additionally, mass balance of many of the events is not equal and is the result of the resolution of the data.

## **4. Results**

### *4.1 Trigger mechanism and flow frequency*

Events inferred to be triggered by settling from river plumes account for 73% of the flow events, while landslides and their associated turbidity currents account for the remaining 27% of events (Fig. 2).

### *4.2 Trigger mechanism and flow behaviour*

The 95 flows that we analyse (Figure 4) exhibit six distinct combinations of behaviour (bypass, deposition, erosion) and trigger (landslide or plume-trigger) (Fig. 2b). All combinations can reach the lobe, which is defined as the area where flow exits the channel and expands.

The most common landslide events display net-bypassing behaviour; near-equal volumes of sediment are eroded from the stoss- and lee-slopes of each bedform, resulting in little net-change in suspended sediment; they have a headscarp of variable volume. The second-most common landslide events are net-depositional; they typically, although not always, result from the largest volume landslides. The cumulative profiles of net-depositional landslide events show exponential decay of cumulative volume, and negligible volumes of erosion in comparison. Net-erosive landslides are relatively rare;



they are highly erosive events that begin with a small headscarp, and tend to occur in conjunction with additional failures along the channel (Supplemental Figure 5).

The most common settling plume events are net-depositional, the second-most common settling plume events exhibit bypassing behaviour, and the least common settling plume events are erosive, accounting for only ~10% of plume events. The erosive plume events have long runout distances, and always reach the channel lobe where they deposit the majority of their sediment. Erosive settling plume events begin to lose erosive power whilst still within the channel, but do not begin to deposit large amounts of sediment until they reach the lobe. Erosive settling plume events tend to coincide with peaks in river discharge (Supplemental Figure 6).

#### *4.3 Trigger mechanism and runout distance*

The longest runout flows are not caused by a single particular trigger (Fig. 2; Fig. 3); although long runout events are usually associated with peaks in river discharge (Supplemental Figure 6). Landslide events show no clear relationship between landslide volume and runout; some of the largest landslides have short runout distances and create channel-plugging deposits (Supplemental Figure 5). Runout distances are affected by channel length, which varies for the northern, southern and central channels (Fig. 3c; d). Additionally, landslide volume could be affected by the delta lip configuration, which varies for the different channels.

In order to consider whether channel length or relative landslide volume has an influence on runout distance, in Figure 3 we show the data in both the absolute and normalised format. The runout length has here been normalised by the channel length, and the landslide volume has been normalised by the maximum observed landslide volume in that channel. The shorter northern and central channels display greater normalised runout distances than the longer southern channel. The scatter in relationship between landslide volume and runout is enhanced by normalising the initial volume and runout. This highlights that shorter channels experience a greater number of events reaching the channel lobe, relative to longer channels.

Settling plume events are the most common turbidity current trigger. Settling plume events are the least effective at reaching the lobe but because of their relative abundance, they contribute the most sediment to the lobe. This highlights the importance of plume events in progradation of the channel-lobe system.

### **5. Discussion**

#### *5.1 Which trigger mechanism forms the most frequent turbidity currents, and transports the most sediment?*

We find that plume events are surprisingly the most frequent turbidity current trigger on the Squamish Delta. Previous work suggests that landslides (Obelcz et al., 2017; Prior et al., 1981) and hyperpycnal flows (Dietrich et al., 2016; Mulder et al., 2003) are the most important turbidity current trigger on deltas (Piper and Normark, 2009). While here we found that plume events and landslides transport similar net-volumes of total sediment during the survey period, depositing 385,000 m<sup>3</sup> and 330,000 m<sup>3</sup> of sediment

respectively. It might be expected that settling plume events would transport less sediment owing to their dilute origins (Parsons et al., 2001), but this is not the case.

### *5.2 Which trigger mechanism reworks sediment the most and has the greatest effect on delta sculpting?*

A lower percentage of plume-triggered events reach the lobe relative to landslide-triggered events. However, plume events are more frequent, produce more erosive flows, and contribute more sediment to the lobe than landslide events. Plume-triggered events therefore rework the most sediment within the time frame of the survey period. This highlights the importance of plume events in lobe-building and channel extension, while landslides largely appear to contribute sediment to the delta front. This is in contrast to the literature that suggests that landslides (Obelcz et al., 2017; Prior et al., 1981) and hyperpycnal flows (Dietrich et al., 2016; Mulder et al., 2003) are the most common sediment transport mechanisms on river deltas.

The apparent mobility of plume-triggered events, relative to landslides may be a result of the initial high density of a landslide-triggered event, compared to the more dilute plume-triggered events. The ability of any turbidity current to erode sediment, and self-accelerate, depends on the near-bed sediment concentration (Eggenhuisen et al., 2017; Parker et al., 1986). Turbulence is dampened if the sediment concentration is too high. Landslides have been shown to struggle to disintegrate and become turbulent (Felix and Peakall, 2006), and these events may deposit most of their sediment or bypass (Sequeiros et al., 2009). As a result, dense landslide-triggered flows may not be able to erode sediment and therefore the volume of sediment in suspension will decay with distance. Overall landslide-triggered turbidity currents rework the bed less, across the survey period, than plume-triggered turbidity currents because they occur less frequently.

### *5.3 The relationship between trigger and turbidity current runout*

We find that the turbidity current trigger does not dictate runout distance. Terrestrial landslides show a strong relationship between increased volume and longer runout (Dade and Huppert, 1998). At the Squamish Delta, events that comprise an initial landslide and associated turbidity current exhibit a poor relationship between volume and runout (Fig. 3). This may be partly because runout distance relates to the ability of the landslide to disintegrate and mix with ambient fluid to form a turbidity current (Felix and Peakall, 2006). The core of larger landslides may be shielded from mixing with ambient water thus inhibiting disaggregation. Smaller landslides may be able to disintegrate more effectively, and produce a turbidity current that can then travel further. However, plume-derived turbidity currents at Squamish Delta commonly exhibit long runouts, although this is partly because they are common in the longer southern channel (Fig. 2; Fig. 3). Long runout plume events also tend to be erosive events. Plume events originate from the dilute river plume (Hughes Clarke et al., 2012), and this low initial concentration may enable them to maintain turbulence that suspends sediment enabling long runout (Sequeiros et al., 2009).

### *5.4 Wider Implications*



It was previously considered that extreme events such as earthquakes (Goldfinger, 2011), river floods (Mulder et al., 2003) and delta-collapses (Girardclos et al., 2007) triggered the large-scale turbidity currents required to build channel lobes. However in this study we find that plume events cause the most seafloor change, contribute the most sediment to the channel lobe, and are most hazardous for seafloor infrastructure, at least over short (3-4 month) timescales. Mechanisms similar to the plume settling process described here have been observed in other locations, including offshore from the Sepik River [Kineke et al., 2000], and Fraser River [Lintern et al., 2016]. Sediment concentrations and fluxes at the Squamish Delta, and Sepik or Fraser Rivers, are not unusual (Supplemental Figure 1). Whilst the frequency and importance of plume-triggered turbidity currents remains to be tested in a wider range of settings, the implications of this work are important. Flows that reach the depositional lobes do not need to be triggered by landslides, earthquakes, or hyperpycnal floods. We show for the first time that settling from surface river plumes can sometimes dominate the triggering of submarine flows, and offshore sediment fluxes.

### **Acknowledgements**

The data used to produce the plots in this paper are available online.

Jamie L. Hizzett is funded jointly by National Environmental and Research Council (NERC) Centre for Doctoral Training (CDT) in Oil and Gas and the University of Southampton.

During the period of data acquisition, John Hughes Clarke was supported by the Natural Sciences and Engineering Research Council (Canada) and the sponsors of the Chair in Ocean Mapping at the University of New Brunswick.

Esther J. Sumner was supported by the Natural Environment Research Council projects NE/M017540/1

Matthieu J.B. Cartigny was supported by the Natural Environment Research Council projects NE/P009190/1, NE/M017540/1 and NE/M007138/1.

Peter J. Talling was supported by the Natural Environment Research Council projects NE/N012798/1, NE/P009190/1, NE/M017540/1 and NE/M007138/1.

Michael A. Clare was supported by the Natural Environment Research Council projects NE/N012798/1 and NE/P009190/1.

We thank the crew of the CSL Heron who collected the data used in this report.

### **References**

- Carter, L., Gavey, R., Talling, P. J., & Liu, J. T. (2014). Insights into submarine geohazards from breaks in subsea telecommunication cables. *Oceanography*, 24(3), 58–67.  
<https://doi.org/10.5670/oceanog.2011.65>
- Clare, M. A., Hughes Clarke, J. E., Talling, P. J., Cartigny, M. J. B., & Pratomo, D. G. (2016).

- Preconditioning and triggering of offshore slope failures and turbidity currents revealed by most detailed monitoring yet at a fjord-head delta. *Earth and Planetary Science Letters*, 450, 208–220. <https://doi.org/10.1016/j.epsl.2016.06.021>
- Dade, W. B., & Huppert, H. E. (1998). Long-runout rockfalls. *Geology*, 26(9), 803–806. [https://doi.org/10.1130/0091-7613\(1998\)026<0803:LRR>2.3.CO](https://doi.org/10.1130/0091-7613(1998)026<0803:LRR>2.3.CO)
- Dietrich, P., Ghienne, J.-F., Normandeau, A., & Lajeunesse, P. (2016). Upslope-Migrating Bedforms In A Proglacial Sandur Delta: Cyclic Steps From River-Derived Underflows? *Journal of Sedimentary Research*, 86(2), 113–123. <https://doi.org/10.2110/jsr.2016.4>
- Eggenhuisen, J. T., Cartigny, M. J. B., & De Leeuw, J. (2017). Physical theory for near-bed turbulent particle suspension capacity. *Earth Surface Dynamics*, 5(2), 269–281. <https://doi.org/10.5194/esurf-5-269-2017>
- Felix, M., & Peakall, J. (2006). Transformation of debris flows into turbidity currents: mechanisms inferred from laboratory experiments. *Sedimentology*, 53(1), 107–123. <https://doi.org/10.1111/j.1365-3091.2005.00757.x>
- Girardclos, S., Schmidt, O., Sturm, M., Ariztegui, D., Pugin, A., & Anselmetti, F. (2007). The 1996 AD delta collapse and large turbidite in Lake Brienz. *Marine Geology*, 241(1), 137–154.
- Goldfinger, C. (2011). Submarine paleoseismology based on turbidite records. *Annual Review of Marine Science*, 3, 35–66.
- Hughes Clarke, J. E. (2016). First wide-angle view of channelized turbidity currents links migrating cyclic steps to flow characteristics. *Nature Communications*, 7(May), 11896. <https://doi.org/10.1038/ncomms11896>
- Hughes Clarke, J. E., Brucker, S., Muggah, J., Hamilton, T., Cartwright, D., Church, I., & Kuus, P. (2012). Temporal progression and spatial extent of mass wasting events on the Squamish prodelta slope. In *Landslides and Engineered Slopes: Protecting Society through Improved Understanding* (Vol. 122, pp. 1091–1096).
- Hughes Clarke, J. E., Marques, C. R. V., & Pratomo, D. (2014). Imaging Active Mass-Wasting and Sediment Flows on a Fjord Delta, Squamish, British Columbia. *Springer International Publishing*, 249–260. <https://doi.org/10.1007/978-3-319-02904-7>
- Kineke, G. C., Woolfe, K. J., Kuehl, S. A., Milliman, J. D., Dellapenna, T. M., & Purdon, R. G. (2000). Sediment export from the Sepik River, Papua New Guinea: Evidence for a divergent sediment plume. *Continental Shelf Research*, 20(16), 2239–2266. [https://doi.org/10.1016/S0278-4343\(00\)00069-8](https://doi.org/10.1016/S0278-4343(00)00069-8)
- Lamb, M. P., & Parsons, J. D. (2005). High-Density Suspensions Formed Under Waves. *Journal of Sedimentary Research*, 75(3), 386–397. <https://doi.org/10.2110/jsr.2005.030>
- Lintern, D. G., Hill, P. R., & Stacey, C. (2016). Powerful unconfined turbidity current captured by cabled observatory on the Fraser River delta slope, British Columbia, Canada. *International Association of Sedimentologists Special Publications*, 1041–1064. <https://doi.org/10.1111/sed.12262>
- Mastbergen, D. R., & Van Den Berg, J. H. (2003). Breaching in fine sands and the generation of sustained turbidity currents in submarine canyons. *Sedimentology*, 50(4), 625–637. <https://doi.org/10.1046/j.1365-3091.2003.00554.x>
- Milliman, J., & Farnsworth, K. (2013). River Discharge to the Coastal Ocean: A Global Synthesis. *Cambridge University Press*, 24(4), 143–160. <https://doi.org/10.5670/oceanog.2011.108>
- Mulder, T., Syvitski, J. P. M., Migeon, S., Faugères, J.-C., & Savoye, B. (2003). Marine hyperpycnal flows: initiation, behavior and related deposits. A review. *Marine and*

- Petroleum Geology*, 20(6–8), 861–882.  
<https://doi.org/10.1016/j.marpetgeo.2003.01.003>
- Mulder, T., & Syvitski, J. P. M. (1995). Turbidity Currents Generated At River Mouths During Exceptional Discharges To the World Oceans. *Journal of Geology*, 103(3), 285–299.
- Normandeau, A., Lajeunesse, P., St-Onge, G., Bourgault, D., Drouin, S. S. O., Senneville, S., & Blanger, S. (2014). Morphodynamics in sediment-starved inner-shelf submarine canyons (Lower St. Lawrence Estuary, Eastern Canada). *Marine Geology*, 357(September), 243–255. <https://doi.org/10.1016/j.margeo.2014.08.012>
- Obelcz, J., Xu, K., Georgiou, I. Y., Maloney, J., Bentley, S. J., & Miner, M. D. (2017). Sub-decadal submarine landslides are important drivers of deltaic sediment flux: Insights from the Mississippi River Delta Front. *Geology*, 45(7), G38688.1. <https://doi.org/10.1130/G38688.1>
- Pantin, H. M. (1979). Interaction between velocity and effective density in turbidity flow: Phase-plane analysis with criteria for autosuspension. *Marine Geology*, 31, 59–99.
- Parker, G., Fukushima, Y., & Pantin, H. M. (1986). Self-accelerating turbidity currents. *J. Fluid Mech.*, 171, 145–181.
- Parsons, J. D., Bush, J. W. M., & Syvitski, J. P. M. (2001). Hyperpycnal plume formation from riverine outflows with small sediment concentrations. *Sedimentology*, 48(2), 465–478. <https://doi.org/10.1046/j.1365-3091.2001.00384.x>
- Piper, D. J. W., & Normark, W. R. (2009). Processes That Initiate Turbidity Currents and Their Influence on Turbidites: A Marine Geology Perspective. *Journal of Sedimentary Research*, 79, 347–362. <https://doi.org/10.2110/jsr.2009.046>
- Prior, D. B., Wiseman, W. J., & Gilbert, R. (1981). Submarine slope processes on a fan delta, Howe Sound, British Columbia. *Geo-Marine Letters*, 1(2), 85–90. <https://doi.org/10.1007/BF02463323>
- Saucier, F. J., & Chassé, J. (2000). Tidal circulation and buoyancy effects in the St. Lawrence Estuary. *Atmosphere-Ocean*, 38(4), 505–556. <https://doi.org/10.1080/07055900.2000.9649658>
- Sequeiros, O. E., Naruse, H., Endo, N., Garcia, M. H., & Parker, G. (2009). Experimental study on self-accelerating turbidity currents. *Journal of Geophysical Research*, 114(C5), C05025. <https://doi.org/10.1029/2008JC005149>
- Shao, Y., Hung, C., & Chou, Y. (2017). Numerical study of convective sedimentation through a sharp density interface. *Journal of Fluid Mechanics*, 824, 513–549. <https://doi.org/10.1017/jfm.2017.349>

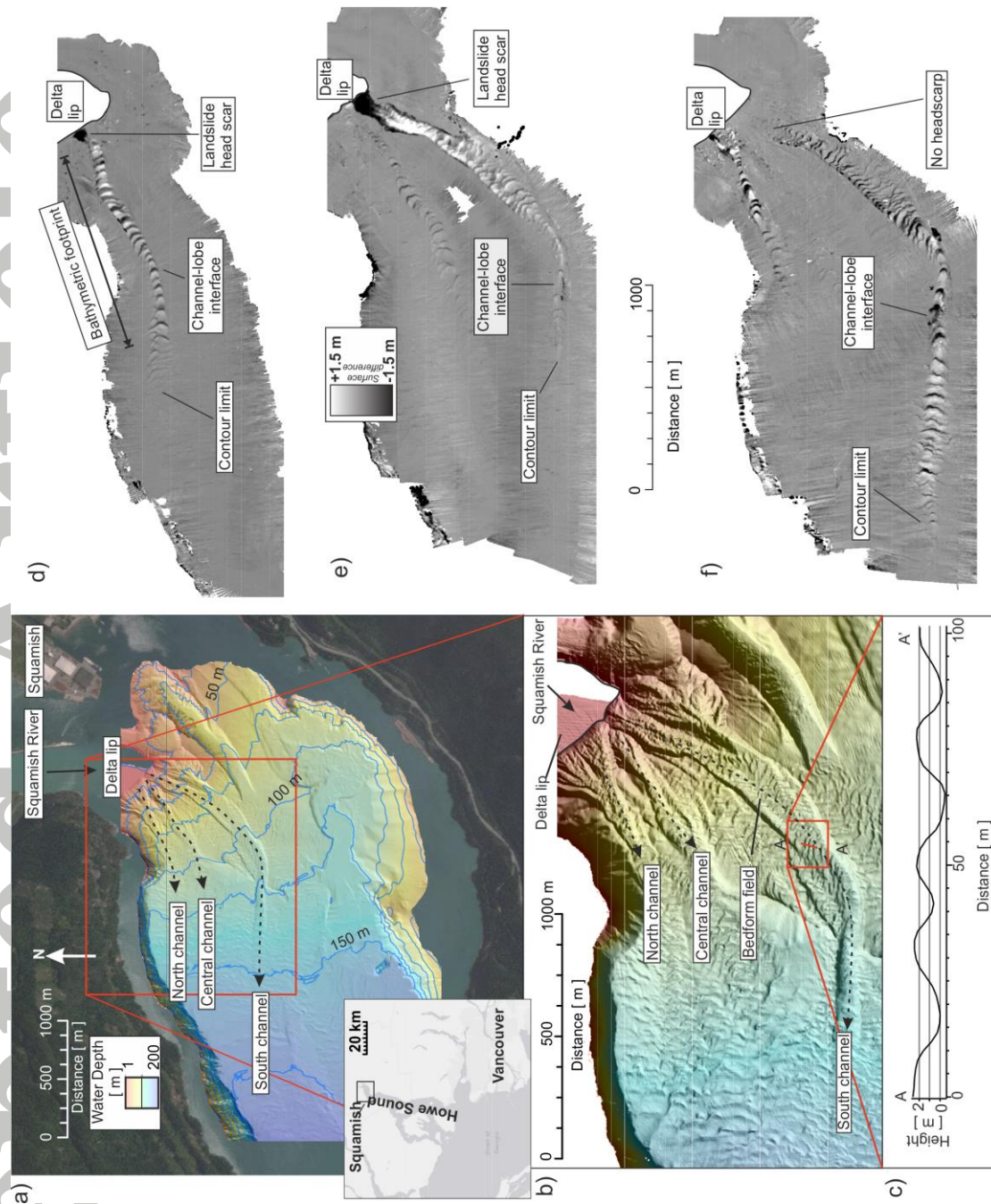


**Figure 1.** **a)** Overview bathymetric map of the Squamish Delta. Inset map shows the location of Squamish Delta. **b)** Bathymetric map of the Squamish Delta showing the channels and associated bedform fields. **c)** The morphology of bedforms on the channel floor. **(d-f)** Changes in seafloor elevation between bathymetric surveys on different days in 2011, showing morphological footprint of individual flows. The white patches indicate areas characterised by deposition in between surveys, while the black patches indicate areas characterised by erosion. **d)** Flow triggered by a small volume landslide ( $\sim 4,000 \text{ m}^3$ ). **e)** Flow triggered by a large volume landslide ( $\sim 22,000 \text{ m}^3$ ). **f)** Flow triggered by sediment setting from a surface plume, which lacks a landslide headscar. Note that the small landslide (d) and the settling plume trigger (e) produce longer runout turbidity current than the large landslide (f).



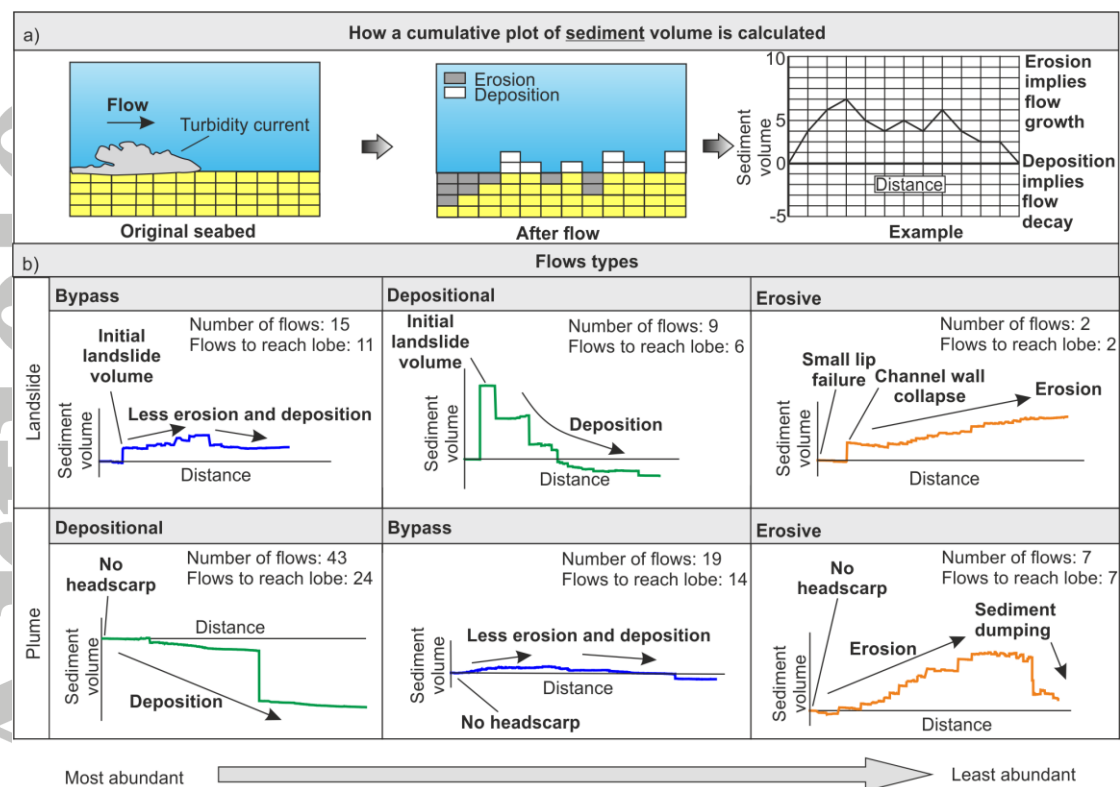


**Figure 2. a)** Explanation of how cumulative plots for turbidity current erosion and deposition patterns are calculated. **b)** Event types classified according to their initial trigger (landslide or settling from plume), and are then ranked by their abundance as either net-depositional, net-bypassing, or net erosional in terms of flow volume. The cumulative profiles depicted are not shown to scale. Flow volume is calculated using the initial landslide volume (plume events start with zero volume), and cumulative amounts of sediment eroded or deposited along the flow pathway. The number of events of each type are noted, as are the number of those events that reach the lobe.



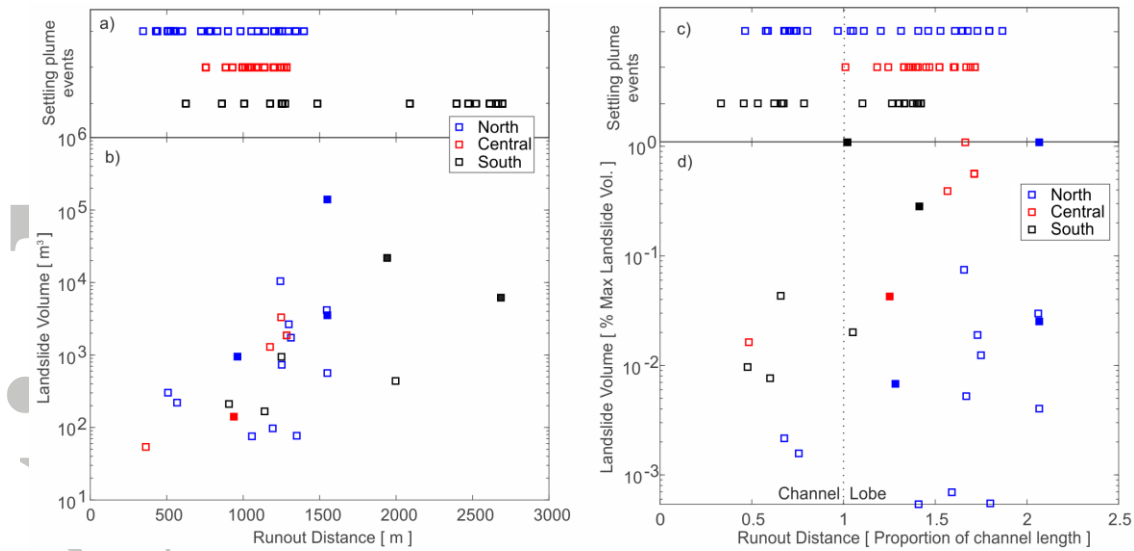


**Figure 3: a)** The runout distance of plume-triggered turbidity currents, which originate from the north, central and southern channels. Note that these three channels have different lengths, and longer channels may favour longer runout. **b)** Relationship between initial landslide volume and runout distance, subdivided for events starting in the north, central and southern channels. **c)** Normalised runout of plume-triggered turbidity currents. **d)** Normalised volume and runout of landslide events. Solid squares indicate a landslide whose initial volume is underestimated due to a missing headwall on one of the survey pairs because the water at the delta lip was too shallow to survey.

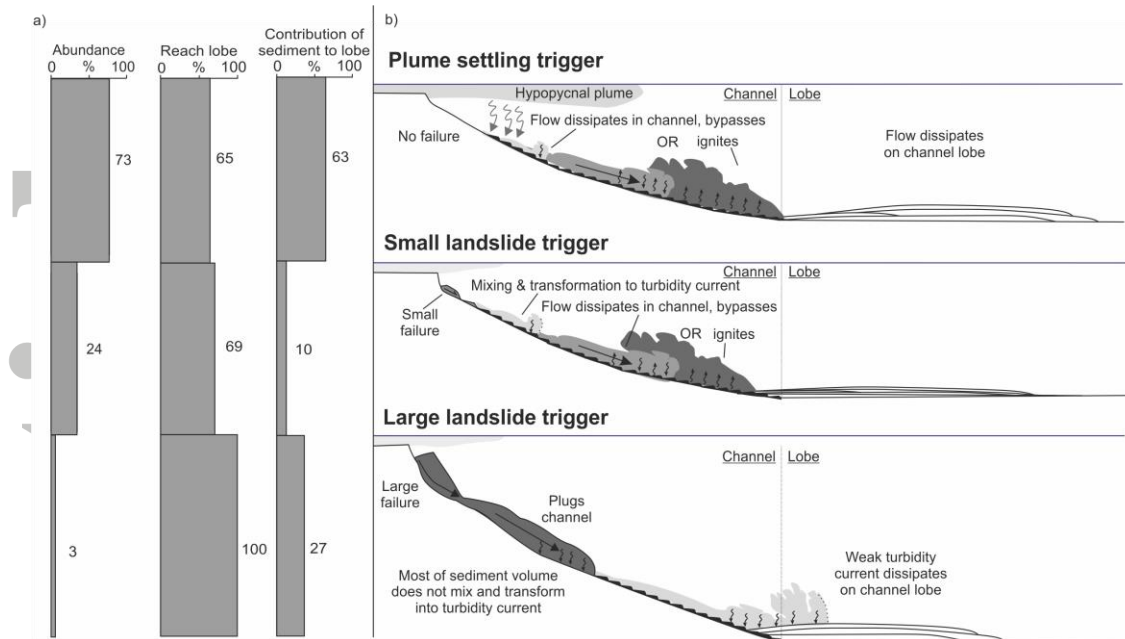


**Figure 4:** A summary of flow behaviours at Squamish Delta. **(a)** The bar charts represent the abundance of flows from plume events (top), small landslides ( $< 10,000 \text{ m}^3$ ) (middle) and large landslides ( $> 10,000 \text{ m}^3$ ) (bottom), percentage of these flows that reach the lobe, and the relative contribution of those flows to deposition on the lobe. **(b)** Cartoons summarising the typical flow evolution of turbidity currents triggered by sediment settling from surface plumes, and by small or large landslides.